



Comparative Performance Analysis of Polylactic Acid Parts Fabricated by 3D Printing and Injection Molding

Ujendra Kumar Komal, Bal Kishan Kasaudhan, and Inderdeep Singh

Submitted: 17 December 2020 / Revised: 17 April 2021 / Accepted: 7 May 2021 / Published online: 20 May 2021

In the present experimental investigation, the specimens were fabricated using 3D printing (fused deposition modeling) and injection molding techniques. The process parameters were optimized to fabricate the good quality polylactic acid (PLA) specimens as per ASTM standards. The effect of variation (80, 90, and 100%) of the infill density on the mechanical performance of developed specimens was analyzed. The mechanical behavior of the fabricated specimens was compared in the context of tensile, flexural, and impact properties. The thermal stability and crystallinity of the PLA specimens have been investigated using thermogravimetric and XRD analysis, respectively. After tensile testing, the surface of the fractured specimens was observed using a scanning electron microscope. The tensile and flexural strength of the 3D-printed specimens was superior to the injection-molded specimens. An improvement in stiffness of the 3D-printed specimens has been observed. Moreover, the printed specimens showed better thermal stability than the molded specimens. There was no significant variation in the crystallinity of the printed and molded specimens. It can be concluded that the tensile, flexural, and thermal responses of the 3D-printed specimens are better than injection-molded specimens at the optimal combination of process parameters.

Keywords 3D printing, FDM, injection molding, mechanical properties, PLA, thermal properties

1. Introduction

Additive manufacturing has revolutionized the new product development cycle by significantly reducing the time frame between the conceptualization of ideas and the launch of tangible products. The application spectrum of various additive manufacturing technologies has slowly shifted from creating prototypes to the fabrication of fully functional products. However, the mechanical performance of the parts/components produced by various layered-manufacturing techniques has been an area of concern and research focus. Also, the time required to create 3D parts using additive manufacturing methods, such as stereolithography (SLA), fused deposition modeling (FDM), is high. In order to compete with the commercial polymer processing methods, such as injection molding, the comparative/higher mechanical performance at a lower cost is expected to tilt the decision in favor of additive manufacturing technologies. The higher cost of the tooling

(mold) in injection molding can only be justified for a significantly large production volume. With the current focus of the industry toward customization and offer variety to the customers, there is a huge potential for employing additive manufacturing for the fabrication of functional products with a high degree of design flexibility. FDM is generally considered the most commonly used additive manufacturing technique for thermoplastics due to its simple working principles, ease of handling, rapid operation, and lower power consumption (Ref 1-3). However, there is a general belief that the parts/components made of the FDM process lack properties due to the formation of voids and air gaps during fabrication. A significant number of investigations focussing on optimizing the operating parameters like raster width and angle, infill orientation, layer height and thickness, and bed temperature have already been reported to enhance the quality of the plastic components (Ref 4, 5). Tymrak et al. (Ref 6) proposed that the raster angle of 0°/90° could be preferred to improve the tensile behavior of the PLA and acrylonitrile butadiene styrene (ABS). Aw et al. investigated the effect of 100% infill density and line pattern on the mechanical behavior of the products. The authors concluded that 100% infill density and line pattern significantly remove the air voids between the layers and improve the adhesion between the layers, leading to improved mechanical properties (Ref 7). The various types of thermoplastics such as PLA, ABS, polycarbonate (PC), and polypropylene (PP) have been used in the FDM process, and their effect on the behavior of the parts/components has been investigated (Ref 8-10). Material selection is at the core of any design innovation. The researchers have widely explored the biopolymers like PLA due to their biodegradability, renewability, and high strength and suggested that it has tremendous potential as a substitute for petroleum-derived polymers for various applications (Ref 11, 12). Form the last few years, PLA has been successfully employed in packaging, industrial, and biomedical applications due to its biodegradability, compostability, and biocompatibility

This invited article is part of a special topical focus in the *Journal of Materials Engineering and Performance* on Additive Manufacturing. The issue was organized by Dr. William Frazier, Pilgrim Consulting, LLC; Mr. Rick Russell, NASA; Dr. Yan Lu, NIST; Dr. Brandon D. Ribic, America Makes; and Caroline Vail, NSWC Carderock.

Ujendra Kumar Komal and **Inderdeep Singh**, Department of Mechanical and Industrial Engineering, Indian Institute of Technology Roorkee, Roorkee, Uttarakhand 247667, India; and **Bal Kishan Kasaudhan**, Department of Chemical Engineering, Indian Institute of Technology Kanpur, Kanpur, Uttar Pradesh 208016, India. Contact e-mail: inderdeep.singh@me.iitr.ac.in.

(Ref 13, 14). The mechanical behavior of PLA parts fabricated using the FDM process has been widely explored (Ref 15-19).

The comparative investigation of the parts fabricated by FDM and injection molding has also been reported in some articles (Ref 3, 20). However, the majority of the literature is focused on the tensile behavior of the polymers. A robust understanding of the comparative performance analysis of the parts manufactured using FDM and injection molding is rarely available.

The judicious selection of materials is essential for ensuring the concept of 'Design for Environment'. Therefore, the sustainable material option, PLA, was selected for the current research endeavor. The current investigation highlights the impact of infill density on the thermal, mechanical, and crystalline behavior of the PLA specimens fabricated using the FDM technique. The comparative performance analysis (in terms of thermal, mechanical, and crystalline) of the parts manufactured using FDM and injection molding has also been conducted.

2. Materials and Methods

2.1 Fused Deposition Modeling (FDM)

The blue-colored PLA filament having a diameter of 1.75mm was purchased from Novabeans, Gurugram, Haryana, India. The PLA specimens were printed according to ASTM D3039, ASTM D7264, and ASTM D256 standards for tensile, flexural, and impact tests, respectively. The specimens with varying infill densities (80, 90, and 100%) were printed using FDM.

2.2 Injection Molding (IM)

The PLA filament was pelletized into an average length of 4-5 mm. These pellets were used to fabricate test specimens using a commercial scale injection molding machine. The details of the process parameters used during both the processes are given in Table 1. Figure 1 depicts the test specimens fabricated using both techniques.

The abbreviations used in Table 1 are; IM = Specimen fabricated using injection molding. D1, D2, and D3 = Speci-

mens fabricated using FDM where D1 = Infill density, 80%, D2 = Infill density, 90%, and D3 = Infill density, 100%.

2.3 Mechanical Performance

The tensile, flexural, and impact test specimens were fabricated as per ASTM D3039, D7264, and D256, respectively. The tensile and flexural behavior of the PLA specimens was investigated in the context of ultimate strength and modulus using a Universal Testing Machine (UTM) (Instron: 5982, USA, Load Cell = 10 kN equipped with Blue Hill Software). Both the tensile and flexural tests were conducted at a loading rate of 2 mm/min. The impact test was conducted using a low energy impact tester.

2.4 Thermal Analysis

The thermal behavior of the specimens was investigated using a thermogravimetric analyzer. Both the thermogravimetric analysis (TGA) and differential thermal analysis (DTA) were executed using the same equipment. A metered sample

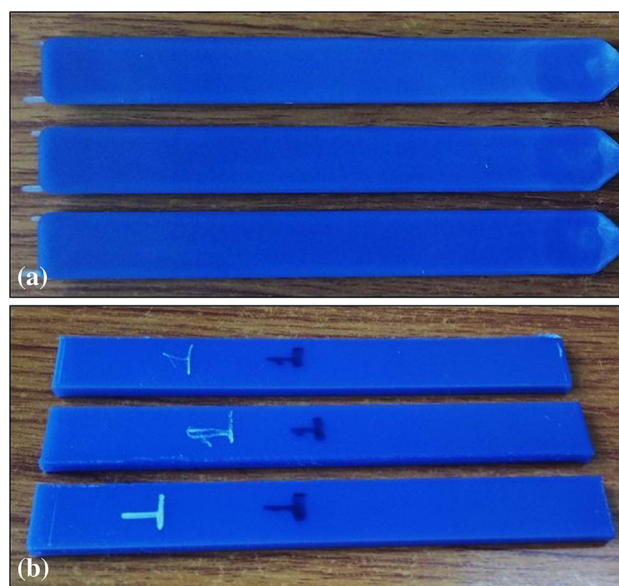


Fig. 1. (a) injection-molded and (b) 3D-printed specimens

Table 1 Details of process parameters

| 3D Printing | | | | Injection molding | |
|--------------------------|------|------|------|-------------------------|--------------------|
| Parameters | D1 | D2 | D3 | Parameters | IM |
| Layer height, mm | 0.1 | 0.1 | 0.1 | Temperature profile | 170-165-160-155 °C |
| Shell thickness, mm | 1.2 | 1.2 | 1.2 | Injection pressure, MPa | 50 |
| Bottom/top thickness, mm | 1 | 1 | 1 | Holding pressure, MPa | 40 |
| Fill density, % | 80 | 90 | 100 | Holding time, s | 15 |
| Print speed, mm/s | 60 | 60 | 60 | Cooling time, s | 30 |
| Printing temperature, °C | 210 | 210 | 210 | | |
| Bed temperature, °C | 50 | 50 | 50 | | |
| Platform adhesion type | Raft | Raft | Raft | | |
| Diameter, mm | 1.8 | 1.8 | 1.8 | | |
| Flow, % | 107 | 107 | 107 | | |
| Nozzle, mm | 0.4 | 0.4 | 0.4 | | |

was placed in a pan and heated from room temperature (25–30 °C) to 600 °C with a heating rate of 5 °C/min. All the tests were conducted in a nitrogen atmosphere, and the loss of mass was recorded with respect to temperature. The data obtained from the test were used to plot the curves and compare the glass transition, crystallization, and melting temperature of the specimens.

2.5 Crystallinity

The XRD analysis was performed using a Bruker diffractometer (D8-Advance) for the angle range (2θ) of 5°–60° with a scanning speed of 1°/min. Copper was used as a target material. The data have been analyzed using X'Pert Highscore software, and the spectra were plotted from the analyzed data using Origin software (Ver. 8.5). The total area under the curve and crystalline area were measured using Origin software. Finally, the crystallinity of the specimens was quantified using Eq 1 suggested by Vonk (Ref 21).

$$\text{Crystallinity (\%)} = \frac{\text{Crystalline area}}{\text{Total area under the curve}} \times 100 \quad (\text{Eq 1})$$

2.6 Microstructural Analysis

The surfaces of fractured specimens were observed using an optical camera and scanning electron microscope (SEM). The specimens' failure characteristics under tensile loading and variation in properties were understood using these images.

3. Results and Discussion

3.1 Mechanical Performance

Mechanical behavior of the injection-molded (IM) and 3D-printed (D1, D2, and D3) specimens was evaluated in the context of tensile, flexural, and impact responses. The data obtained from the tests were plotted, as shown in Figs. 2 and 3. All the specimens demonstrated a brittle failure during tensile testing. The mechanical properties of 3D-printed specimens' mechanical properties were found to increase with infill density, and maximum properties were recorded for D3. The increase in

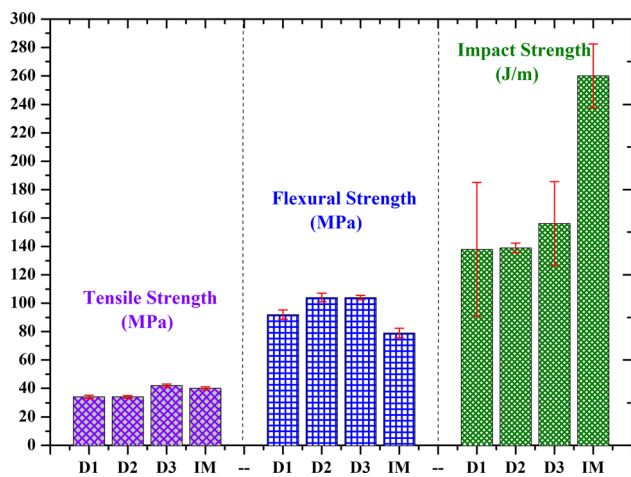


Fig. 2. Variation in mechanical strength

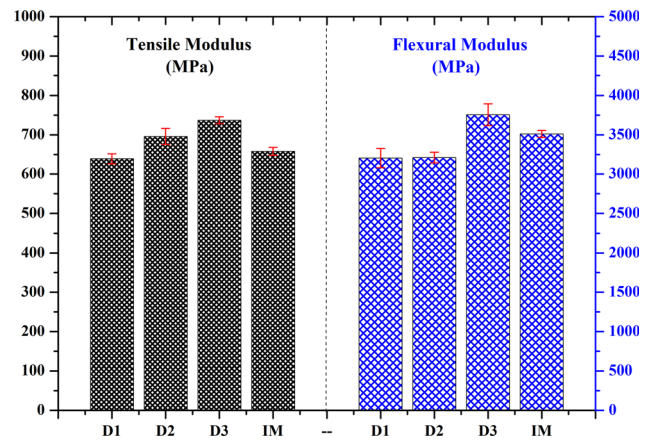


Fig. 3. Variation in modulus

strength (tensile, flexural, and impact) with higher infill density is attributed to the strong bond created between the rasters, which required a comparative higher force to break. Similar types of observation have also been reported previously (Ref 22, 23). The increment in tensile and flexural modulus with infill density is correlated with the improvement in stiffness of the PLA. The improvement in modulus is due to the comparative lower voids and lower porosity present in the specimens. Moreover, the clustered strands in a single direction arrest the plastic deformation leading to an increase in the stiffness of PLA specimens. A similar trend of variation in modulus with infill density was also reported by Carneiro et al. (Ref 22).

The tensile and flexural responses (strength and modulus) of D3 were recorded higher than the IM specimens. The improvement in properties is due to the strong bonding between the rasters and the presence of clusters of strands. Moreover, the unique direction of the raster throughout the printing improves the polymer molecules' orientation, which also contributes to improving these properties. The lower tensile and flexural properties of IM can also be due to the heterogeneous orientation of polymeric molecules during injection molding. Near the mold surfaces, the polymer molecules align in flow direction and randomly at the core regions, leading to a decrease in the specimens' load-bearing capabilities. The variation in the orientation of polymeric molecules near the surface and core regions is due to the variation in friction force (higher near the mold surfaces and lower at the core regions) during injection molding (Ref 24). Moreover, the degradation of the PLA due to high shearing action during pelletizing and injection molding could be the reason for the reduction in tensile and flexural properties.

Contrary to tensile and flexural strength, the impact strength of the 3D-printed specimen was found to be lower than the IM. This reduction in the impact strength of 3D-printed specimens could be due to the poor fusion between the layers due to lower bed temperature. When the bed temperature decreases, the interlayer temperature at the fusion sites also decreases. At lower temperature, the mobility of the polymeric chain decreases. Therefore, the inter-diffusion between the layers becomes difficult (Ref 25). Moreover, when the temperature at which the diffusion starts is lower, there is less time available for inter-diffusion between the layers before solidification (reaching glass transition temperature). This improper inter-diffusion between the layers resulted in the smaller number of

entangled polymeric molecules between the layers, which resulted in poor adhesion between the layers, and ultimately leading to poor impact resistance (Ref 25).

The finding is also in line with the findings reported by Aliheidari et al. (Ref 25). The authors investigated and concluded that the increase in nozzle and bed temperature increases the fracture resistance of the 3D-printed parts. Benwood et al. (Ref 19) recently suggested that the optimum temperature of bed while printing the PLA should be 105 °C. Moreover, the loading direction (transverse with respect to raster) during the impact test can be another cause for the reduction in impact strength.

3.2 Thermal Properties

The thermal behavior of the PLA was investigated by calculating the loss of mass with respect to temperature. The data obtained from the test have been plotted, as shown in Fig. 4(a) and (b). The TGA curves for all the specimens showed a single-stage degradation, which confirms the absence of fillers or compound in the filament. All the specimens degraded completely around 450 °C. The shifting of the curves on the right-hand side indicates the increase in thermal stability of the specimens with infill density. It can also be confirmed from the data ($T_{5\%}$) presented in Table 2. However, this shifting of curves can be seen only after 250 °C.

The improvement in thermal stability of the specimens with infill density may be attributed to the reduction in air gaps and moisture absorption within the specimens. It is in agreement with the optical images (Fig. 6) and SEM images (Fig. 7). The investigation revealed a reduction in the thermal stability of IM than D1, D2, and D3. It could be attributed to PLA's degradation during pelletizing and injection molding due to high shearing action.

The DTA traces specifically emphasizing the glass transition (T_g), crystallization (T_c), and melting (T_m) temperature are shown in Fig. 4(b). The DTA curves show almost similar traces for all the specimens. The essential data were extracted and are presented in Table 2. It depicts an insignificant change in T_g , T_c , and T_m of all the specimens. The results shown in Table 2 are in line with the previously reported results (Ref 18, 26).

3.3 Crystallinity

The crystallinity of the specimens plays an essential role in understanding the mechanical behavior of polymers and polymer-based composites. The XRD analysis was conducted to observe the variation in crystallinity of the specimens. The degree of crystallinity (%) was found to be 4.93, 4.68, 5.41, and 4.10 for IM, D1, D2, and D3, respectively. The lower crystallinity for all the specimens confirms the highly amorphous nature of PLA. No significant variation in the crystallinity was observed for all the specimens, which indicates that the fabrication techniques used in the current investigation have no significant influence on the crystallinity. The specimens' lower crystallinity is evident by the absence of any sharp peak in the XRD spectra (Fig. 5). The broader peak at $2\theta = 16.5^\circ$ confirms the amorphous region, which is in agreement with the previously reported results (Ref 3, 24).

3.4 Microstructural Analysis

The images taken of the tensile fractured surfaces using an optical camera and SEM are shown in Fig. 6 and 7, respectively. All the specimens show a brittle failure during tensile loading. Figure 6 and 7 also confirm that there is no extensive yielding before failure.

The SEM images (Fig. 7) also revealed good printing with good interlayer and intralayer bonding, which can be the reason for the good mechanical properties of the 3D-printed specimens. The formation of air gaps can be seen between the beads in the 3D-printed specimens which is due to printing orientation and lower infill density. However, a reduction in size and

Table 2 Key observations from TGA and DTA data

| Specimen | T_g , °C | T_c , °C | T_m , °C | $T_{5\%}$, °C |
|----------|------------|------------|------------|----------------|
| IM | 51.34 | 91.07 | 169.15 | 288.39 |
| D1 | 51.77 | 90.69 | 168.88 | 308.59 |
| D2 | 52.63 | 92.53 | 171.67 | 327.57 |
| D3 | 53.28 | 93.58 | 171.41 | 340.67 |

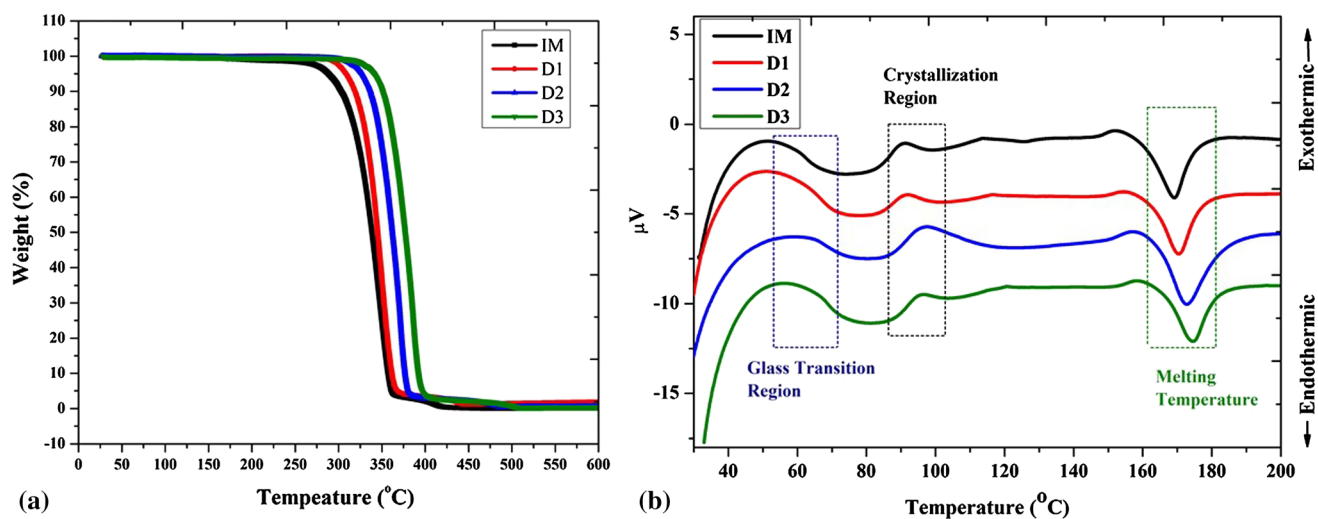


Fig. 4. (a) TGA and (b) DTA curves of the specimens

intensity of air gaps or voids with the increase in infill density was observed. This also confirms that the mechanical properties of the 3D-printed specimens increase with the decrease in air gaps or voids.

The injection-molded specimens show (Fig. 7a) a smooth surface indicating no air gaps. However, the reasons for the lower tensile and flexural properties of IM specimens as compared to D3 specimens have already been explained in sect. 3.1. The fractured surface of the D3 specimens (Fig. 7d)

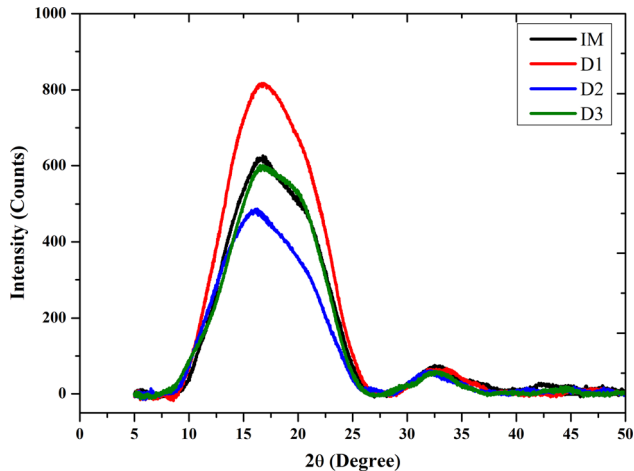


Fig. 5. XRD spectra of the specimens

looks almost similar to the fractured surface of IM specimens (Fig. 7a) due to 100% infill density. The illustrative information generated from the SEM images substantiates the variation in mechanical properties of the specimens.

4. Conclusions

The conventional injection molding process and advanced additive manufacturing technique, i.e., FDM, were used to fabricate good quality PLA specimens as per ASTM standards. To further strengthen the research and industrial fraternity's motivation to adopt additive manufacturing over the conventional methods of fabricating polymeric parts, a comparative performance analysis of the PLA specimens fabricated using injection molding and FDM processes was conducted. Based on the current investigation, it can be concluded that the tensile, flexural, and thermal responses of the 3D-printed specimens at the optimal combination of process parameters are better than injection-molded specimens. However, the impact strength of the injection-molded specimen was superior to the 3D-printed specimens. It can also be suggested that the inorganic and organic fillers can be incorporated while fabricating the filament for FDM to improve the impact strength of the final parts/products. Injection molding and FDM seems to have no significant influence on the crystallinity of the PLA. The current investigation also highlights that the 3D-printed products

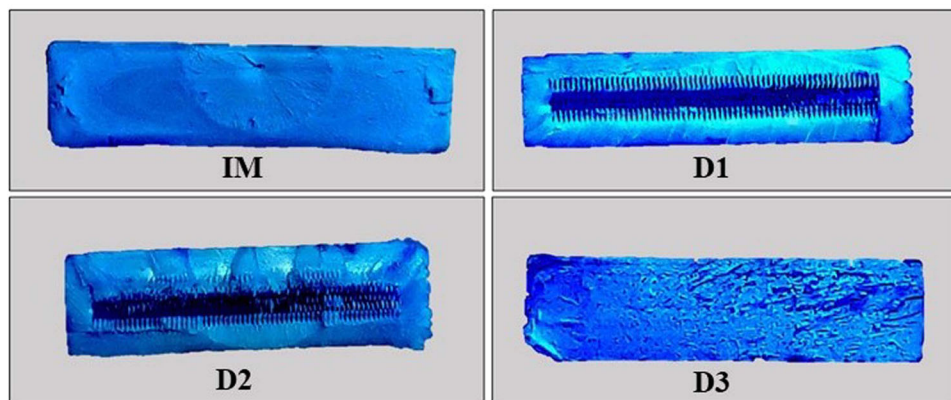
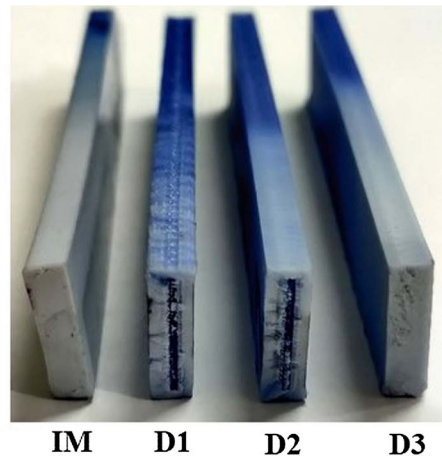


Fig. 6. Optical images of the tensile fractured surfaces

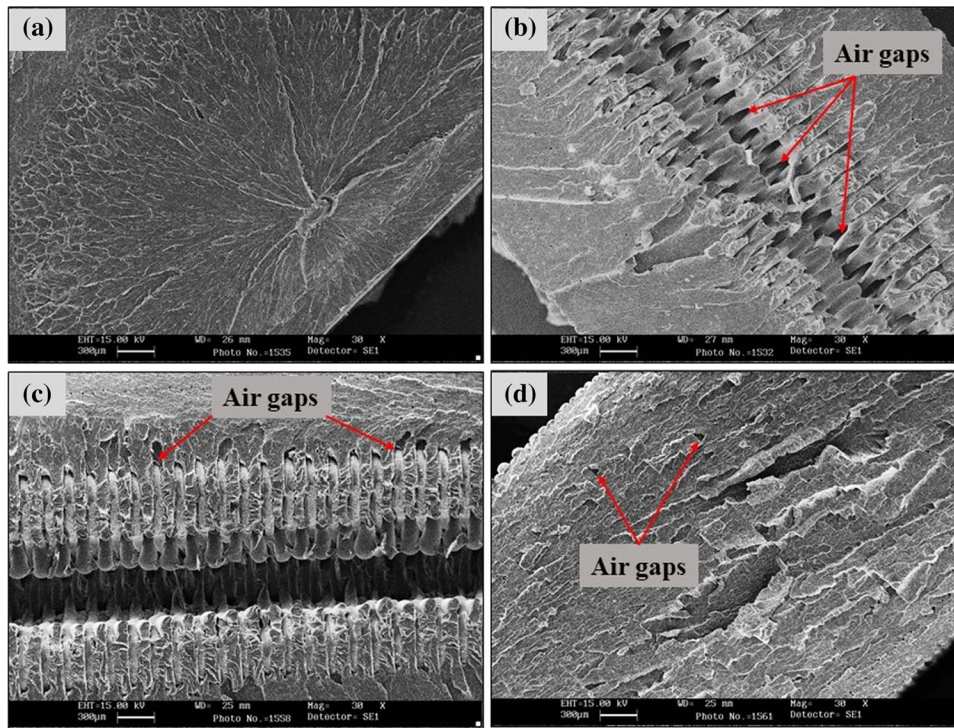


Fig. 7. SEM images of (a) IM (b) D1 (c) D2 and (d) D3 specimens

having lower infill density (80-90%) can also compete with the injection-molded products for various applications.

References

- P. Bettini, G. Alitta, G. Sala and L. Di Landro, Fused Deposition Technique for Continuous Fiber Reinforced Thermoplastic, *J. Mater. Eng. Perform.*, 2017, **26**(2), p 843–848
- J.W. Stansbury and M.J. Idacavage, 3D Printing with Polymers: Challenges among Expanding Options and Opportunities, *Dent. Mater.*, 2015, **32**(1), p 54–64
- M. Lay, N. Laila, N. Thajudin, Z. Ain, A. Hamid, A. Rusli, M. Khalil and R. Khimi, Comparison of Physical and Mechanical Properties of PLA, ABS and Nylon 6 Fabricated Using Fused Deposition Modeling and Injection Molding, *Compos. Part B*, 2019, **176**, p 107341
- A. Lanzotti, M. Grasso, G. Staiano and M. Martorelli, The Impact of Process Parameters on Mechanical Properties of Parts Fabricated in PLA with an Open-Source 3-D Printer, *Rapid Prototyp. J.*, 2015, **21**(5), p 604–617
- A. Rodríguez-Panes, J. Claver and A.M. Camacho, The Influence of Manufacturing Parameters on the Mechanical Behaviour of PLA and ABS Pieces Manufactured by FDM: A Comparative Analysis, *Materials (Basel)*, 2018, **11**(8), p 1333
- B.M. Tymrak, M. Kreiger and J.M. Pearce, Mechanical Properties of Components Fabricated with Open-Source 3-D Printers under Realistic Environmental Conditions, *Mater. Des.*, 2014, **58**, p 242–246
- Y.Y. Aw, C.K. Yeoh, M.A. Idris, P.L. Teh, K.A. Hamzah and S.A. Sazali, Effect of Printing Parameters on Tensile, Dynamic Mechanical, and Thermoelectric Properties of FDM 3D Printed CABS/ZnO Composites, *Materials (Basel)*, 2018, **11**(4), p 466
- O.S. Carneiro, A.F. Silva and R. Gomes, Materials & Design Fused Deposition Modeling with Polypropylene, *Mater. Des.*, 2015, **83**, p 768–776
- N. Hill and M. Haghi, Deposition Direction-Dependent Failure Criteria for Fused Deposition Modeling Polycarbonate, *Rapid Prototyp. J.*, 2014, **20**(3), p 221–227
- Y. Li, S. Gao, R. Dong, X. Ding and X. Duan, Additive Manufacturing of PLA and CF/PLA Binding Layer Specimens via Fused Deposition Modeling, *J. Mater. Eng. Perform.*, 2018, **27**(2), p 492–500
- P.K. Bajpai, I. Singh and J. Madaan, Development and Characterization of PLA-Based Green Composites, *J. Thermoplast. Compos. Mater.*, 2014, **27**(1), p 52–81
- S. Chaitanya, I. Singh and J. Song II., Recyclability Analysis of PLA/Sisal Fiber Biocomposites, *Compos. Part B Eng.*, 2019, **173**, p 106895
- Z. Yang, H. Peng, W. Wang and T. Liu, Crystallization Behavior of Poly(ϵ -Caprolactone)/Layered Double Hydroxide Nanocomposites, *J. Appl. Polym. Sci.*, 2010, **116**(5), p 2658–2667
- S. Saeidlou, M.A. Huneault, H. Li and C.B. Park, Poly(Lactic Acid) Crystallization, *Prog. Polym. Sci.*, 2012, **37**(12), p 1657–1677
- Y. Song, Y. Li, W. Song, K. Yee, K.Y. Lee and V.L. Tagarielli, Measurements of the Mechanical Response of Unidirectional 3D-Printed PLA, *Mater. Des.*, 2017, **123**, p 154–164
- X. Wang, M. Jiang, Z. Zhou, J. Gou and D. Hui, 3D Printing of Polymer Matrix Composites: A Review and Prospective, *Compos. Part B Eng.*, 2017, **110**, p 442–458
- C. Abeykoon, P. Sri-Amphorn and A. Fernando, Optimization of Fused Deposition Modeling Parameters for Improved PLA and ABS 3D Printed Structures, *Int. J. Light. Mater. Manuf.*, 2020, **3**(3), p 284–297
- G. Cicala, D. Giordano, C. Tosto, G. Filippone, A. Recca and I. Blanco, Polylactide (PLA) Filaments a Biobased Solution for Additive Manufacturing: Correlating Rheology and Thermomechanical Properties with Printing Quality, *Materials (Basel)*, 2018, **11**(7), p 1191
- C. Benwood, A. Anstey, J. Andrzejewski, M. Misra and A.K. Mohanty, Improving the Impact Strength and Heat Resistance of 3D Printed Models: Structure, Property, and Processing Correlations during Fused Deposition Modeling (FDM) of Poly(Lactic Acid), *ACS Omega*, 2018, **3**(4), p 4400–4411
- M.D. Zandi, R. Jerez-Mesa, J. Lluna-Fuentes, J. Jorba-Peiro and J.A. Travieso-Rodríguez, Study of the Manufacturing Process Effects of Fused Filament Fabrication and Injection Molding on Tensile Properties of Composite PLA-Wood Parts, *Int. J. Adv. Manuf. Technol.*, 2020, **108**(5–6), p 1725–1735
- C.G. Vonk, Computerization of Ruland's X-Ray Method for Determination of the Crystallinity in Polymers, *J. Appl. Crystallogr.*, 1973, **6**(2), p 148–152
- O.S. Carneiro, A.F. Silva and R. Gomes, Fused Deposition Modeling with Polypropylene, *Mater. Des.*, 2015, **83**, p 768–776

23. B. Liseli, M. Guha and H. Marie, Study of Infill Print Design on Production Cost-Time of 3D Printed ABS Parts, *Int. J. Rapid Manuf.*, 2015, **5**, p 308–319
24. U.K. Komal, M.K. Lila and I. Singh, PLA/Banana Fiber Based Sustainable Biocomposites: A Manufacturing Perspective, *Compos. Part B Eng.*, 2020, **180**, p 107535
25. N. Aliheidari, R. Tripuraneni, C. Hohimer, J. Christ, A. Ameli and S. Nadimpalli, The Impact of Nozzle and Bed Temperatures on the Fracture Resistance of FDM Printed Materials, *Behav. Mech. Multi-funct. Mater. Compos.*, 2017, **10165**, p 1016512
26. Y. Tao, H. Wang, Z. Li, P. Li and S.Q. Shi, Development and Application Of wood Flour-Filled Polylactic Acid Composite Filament for 3d Printing, *Materials (Basel)*, 2017, **10**(4), p 1–6

Publisher's Note Springer Nature remains neutral with regard to jurisdictional claims in published maps and institutional affiliations.